Research Article | Vol. 25, No. 26 | 25 Dec 2017 | OPTICS EXPRESS 32457
Optics EXPRESS

Control of Q-switched laser radiation characteristics via changing the gain distribution

V. V. KIYKO,[1,2,*] S. V. GAGARSKIY,[2] V. V. NAZAROV,[2] A. N. SERGEEV,[2] AND I. CH. BUCHVAROV[2,3]

[1]*Hypermemo Oy, Lylykoskentie 12b, Joensuu 80130, Finland*
[2]*ITMO University, 49 Kronverksky Pr., St. Petersburg 197101, Russia*
[3]*Physics Department, Sofia University "St. Kliment Ohridski", 5 J.Bouchier Blvd.,1164 Sofia, Bulgaria*
**vvkiyko62@gmail.com*

Abstract: The advantages of simultaneous side and end diode pumping of Nd:YAG laser to enhance the spatio-temporal characteristics in the Q-switched mode of operation has been demonstrated. It has been shown that using a hybrid pump geometry in a short linear resonator provides a superior combination of output beam optical quality, energy, and pulse duration in contrast to the solitary use of an end-pump or a side-pump scheme at similar levels of average output power. We have demonstrated a compact single active rod Nd:YAG laser design in Q-switching mode with a pulse duration of 18 ns, pulse energy up to 3mJ, a repetition rate of 8 kHz, and M^2 <2.

OCIS codes: (140.3580) Lasers, solid-state; (140.3540) Lasers, Q-switched; (140.4780) Optical resonators.

References and links

1. R. Iffländer, *Solid-State Lasers for Materials Processing: Fundamental Relations and Technical Realizations* (Springer Series in Optical Sciences, 2001), Vol. **77**.
2. M. N. Zervas and C. A. Codemard, "High Power Fiber Lasers: A Review," STQE **20**(5), 0904123 (2014).
3. J. Speiser, "History, principles and prospects of thin-disk lasers" (German Aerospace Center Institute of Technical Physics, 2014), http://elib.dlr.de/94106/1/Speiser_thin_disk_hist_scaling.pdf.
4. S. G. Grechin and P. P. Nikolaev, "Diode-side-pumped laser heads for solid-state lasers," Quantum Electron. **39**(1), 1–17 (2009).
5. B. Oreshkov, K. Georgiev, S. Gagarskiy, V. Rusov, N. Belashenkov, A. Trifonov, and I. Buchvarov, "High Energy, High Repetition Rate, Q-Switched Diode Pumped Nd:YAG Laser Using an Unstable Resonator with Variable Reflectivity Mirror", (CLEO EUROPE, 2017), Book of Abstracts, p.17.
6. N. N. Du Keming, J. Xu, J. Giesekius, P. Loosen, and R. Poprawe, "Partially end-pumped Nd:YAG laser with a hybrid resonator," Opt. Lett. **23**(5), 370–372 (1998).
7. W. A. Clarkson, N. S. Felgate, and D. C. Hanna, "Simple method for reducing the depolarization loss resulting from thermally induced birefringence in solid-state lasers," Opt. Lett. **24**(12), 820–822 (1999).
8. S. Mondal, S. P. Singh, K. Hussain, A. Choubey, B. N. Upadhyay, and P. K. Datta, "Efficient depolarization-loss-compensation of solid state lasers using only a Glan-Taylor polarizer," Opt. Laser Technol. **45**, 154–159 (2013).
9. J. Sherman, "Thermal compensation of CW-pumped Nd:YAG laser," Appl. Opt. **37**(33), 7789–7796 (1998).
10. J. J. Morehead, "Compensation of laser thermal depolarization using free space," STQE **13**(3), 498–501 (2007).
11. W. C. Scott and M. de Wit, "Birefringence compensation and TEM00 mode enhancement in a Nd:YAG laser," Appl. Phys. Lett. **18**(1), 3–4 (1971).
12. M. Ouhayoun, M. Boucher, O. Musset, and J. P. Boquillon, "A Nd:YAG laser with a vectorial phase conjugate mirror in the gain medium", in *Conference on Lasers and Electro-Optics Europe*, France, 10–15 Sept. 2000, paper CTuN3.
13. P. K. Mukhopadhyay, K. Ranganathan, S. K. Sharma, P. K. Gupta, and T. P. S. Nathan, "Experimental study of simultaneous end-pumping to a diode-side-pumped intracavity frequency doubled Q-switched Nd:YAG laser," Opt. Commun. **256**(1-3), 139–148 (2005).
14. H. Kogelnik and T. Li, "Laser Beams and Resonators," Appl. Opt. **5**(10), 1550–1567 (1966).
15. W. Koehner, *Solid-State Lasers* (Springer Verlag US, 2008).
16. S. De Silvestri, P. Laporta, and V. Magni, "Novel stability diagrams for continuous-wave solid-state laser resonators," Opt. Lett. **11**(8), 513–515 (1986).
17. O. Svelto, *Principels of Lasers* (Springer Verlag US, 2010), Chap.5.

#307970 https://doi.org/10.1364/OE.25.032457
Journal © 2017 Received 26 Sep 2017; revised 20 Nov 2017; accepted 20 Nov 2017; published 13 Dec 2017

Optics EXPRESS

18. Y. V. Shen, T. M. Huang, C. F. Kao, C. L. Wang, and C. S. Wang, "Optimization in scaling fiber- coupled laser-diode end-pumped lasers to higher power: Influence of thermal effect," STQE **33**(8), 1424–1429 (1997).
19. J. K. Jabczynski, K. Kopczynski, and A. Szczesniak, "Thermal lensing and thermal aberration investigations in diode-pumped lasers," Opt. Eng. **35**(12), 3572–3578 (1996).
20. A. Y. Vinokhodov, M. S. Krivokorytov, Y. V. Sidelnikov, V. M. Krivtsun, V. V. Medvedev, and K. N. Koshelev, "High brightness EUV sources based on laser plasma at using droplet liquid metal target," Quantum Electron. **46**(5), 473–480 (2016).

1. Introduction

Q-switched lasers are widely used for many research and technological applications such as precision surface treatment, engraving, micro- and nano-scale surface structuring/patterning, laser peening etc. Various demanding applications requires high average power and high peak power (on the order of hundreds of kilowatts up to several megawatts [1]), as well as a excellent optical beam quality. Many different solutions for selective and non-selective pumping of laser active elements have been suggested and realized to date to fulfill simultaneously the above criteria. The most impressive progress in developing sources with the output power on the order of several watts, up to tens of kilowatts and good output beam quality has been achieved in fiber lasers with a diode pumping [2]. However, achieving a high peak power in compact and low-cost Q-switched all-optical-fiber laser system is practically impossible. High pulse energy and peak power are limited by non-linear processes (in particular, the cascade frequency conversion via Raman scattering) and laser-induced damage of surfaces and the fiber material itself.

An average output power of tens of kilowatts level is achieved also in diode-pumped solid-state lasers (DPSSL) based on disc active elements [3]. However, the peak power of these lasers in Q-switched mode is limited by the amplified spontaneous emission (ASE) in direction perpendicular to the lasing axis.

State of the art systems lasing with both high peak and high average power rely on master oscillator (semiconductor, microchip- or minilaser with short rezonator) operating at high repetition rate with multistage and multipass amplification stages (master-oscillator power amplifier (MOPA) systems). This direction leads to rather complex and expensive laser systems. Besides, the amplification is usually accompanied by the beam quality deterioration due to thermo-optical distortions in the laser amplifier. Moreover, amplification-based systems could benefit by use of maximum possible pulse energy at the input of amplifying stages. So using of powerful master oscillator allows to decrease the number of the amplifying stages and therefore to simplify the MOPA system.

In order to achieve a low beam divergence, and consequently, a high intensity of the output radiation in short-base lasers, various techniques are used in addition to the traditional intra-cavity telescopes. There are a number of different methods for addressing gain coefficient distributions in transverse direction [4,5], or implementation of hybrid resonator setups [6]. The heat transfer problems accompanying generation of a medium to high output powers are solved by various techniques for compensation of thermo-optical distortions in active elements [7–12].

When laser pulse repetition rates exceed the inverse fluorescence lifetime of the laser transition, master oscillators with continuous pumping (continues wave (CW) pump mode) are usually used. For a number of applications the laser should operate in a high-frequency pulsed-periodical mode when the maximum achievable pulse energy at the shortest possible pulse duration is required. To achieve this goal in Q-switched operation mode, the gain factor of the active medium should be well above the lasing threshold at the moment when the generated pulse starts and the cavity roundtrip time (i.e. cavity optical length) should be as short as possible. The first requirement can be achieved either by increasing the pump level per unit of resonator length (which is limited by thermal fracture threshold) or by increasing the active medium length (e.g. by adding more pumped active elements into the resonator).

Optics EXPRESS

However, it leads to the increase of the resonator's optical length with following increase of the cavity round trip time and consequently of the pulse duration.

An alternative method to achieve simultaneously high average and peak power with relatively short pulse duration and high beam brightness is to combine transverse- and longitudinal diode pumping of the active rod. This approach benefits for getting advantages of the both pump laser technologies. In this scenario, a local zone is created along the axis of the active rod where the pump density and corresponding gain coefficient are much higher than when averaged over the active element's total cross-section. When the intracavity modulator is opened, the pulse generation starts exactly within this region, and since the gain coefficient there significantly exceeds the threshold value, the pulse duration should be rather short. Due to the specific design of the resonator, this pulse expands transversely over the total cross-section of the active medium until the saturation energy is reached. The peripheral regions of the active medium should stay lower a steady state lasing threshold. Under this condition the transverse distribution of the output radiation is expected to correlate with that of the seed pulse formed in the paraxial region. A similar approach was used in a Q-switched Nd:YAG green laser using intra-cavity frequency doubling in KTP [13]. However, this experimental study was focused mostly on the enhancement of the green output power by adding properly adjusted longitudinal pump power in the end-pump channel. Despite the apparent simplicity of the suggested approach, its feasibility is not obvious because of non-homogeneous distribution of the imaginary part of the complex refraction index in the laser's active element in the presence of several competing processes, namely, pumping, absorption saturation and lasing. Hence, in order to achieve optimum parameters of the laser output in Q-switched mode of operation with simultaneous transverse- and longitudinal diode pumping of an active element a more comprehensive analysis is required.

Here, we report the results of numerical simulation of the suggested approach and the experimental realization with commercially available components is presented as well.

2. Analysis of the stability regions for a resonator with hybrid pumping

The "hybrid pumping" assumes that the following two zones can be distinguished within the active element when end-pump and side-pump are used together:

- A paraxial zone corresponding to the diameter of the beam of the longitudinal pump, where the action of both the end-pump and side-pump is combined;

- A peripheral zone, where only the side-pump is present.

In the simplest case of an empty linear resonator its geometry is determined by the optical base L_b and the radii of curvature of the rear mirror and output coupler (R1 and R2, respectively) [14]. In the absence of the pump radiation, the positions of the initial points in the stability diagram are given by the parameters $g1_0 = 1 - L_b / R1$ and $g2_0 = 1 - L_b / R2$. The approaches necessary to analyze resonators that contain additional intracavity components with optical power were discussed in [14–17]. The homogeneous side-pump creates a thick lens extending over the total active element. It can be approximated to a reasonable accuracy by a thin parabolic lens with the principal planes located in the vicinity of the active rod center [14,15]. A one-sided end-pump creates a region with optical pass distance difference in radial direction [18-19]. Usually, it is located near the pumped end of the active element and extends only over a fraction of its aperture.

In the case of simultaneous diode-end-pumping and diode-side-pumped active rod the conditions for the formation of the output radiation caustic are different for the paraxial and the peripheral zones. The conditions are determined both by the combination of the parameters $g1_0$, $g2_0$ and the parameters of thermally induced lenses which are result of the transverse distribution of the field in end and side pump respectively.

Optics EXPRESS

The conditions are determined both by the combination of the parameters $g1_0$, $g2_0$ and the parameters of two or more thermally induced lenses with different optical pass distance distributions.

The analysis of the stability of the resonators with the ray transfer matrix technique shows that the values of the modified resonator parameters g1 and g2 depend on the refracting power of the lenses caused by the end- and side-pump (D_e and D_s respectively) and the distances between the lenses and the resonator mirrors. The focal length of these thermal lenses $F_e = D_e^{-1}$, $F_s = D_s^{-1}$ and the localization of the principal planes are determined by the distribution of the absorbed pump power in the active elements as well as by thermo-physical and thermo-optic characteristics of the laser medium and the peculiarities of the design of the particular cooling system. Using the matrix approach [17] the parameters g1 and g2 can be estimated with the following expressions:

$$g1 = D_E \cdot \left(z_S + z_E\right) \cdot \left[1 - \frac{z_D}{R1}\right] + D_S \cdot z_D \cdot \left[1 - \frac{z_E + z_S}{R1}\right] - \frac{z_D + z_E + z_S}{R1} + 1 \qquad (1a)$$

$$g2 = D_E \cdot z_D \cdot \left[1 - \frac{z_E + z_S}{R2}\right] + D_S \cdot \left(z_E + z_S\right) \cdot \left[1 - \frac{z_D}{R2}\right] - \frac{z_D + z_E + z_S}{R2} + 1 \qquad (1b)$$

where D_e and D_s are the optical powers of the lenses induced by the action of the end-pump and side-pump, respectively;

z_E is the distance from the back mirror with a radius of curvature R1 to the first principal plane of the thermal lens D_E,

z_D is the distance between the second principal plane of the thermal lens D_e and the first principal plane of the thermal lens D_S,

z_S is the distance between the second principal plane of the lens D_S and the output coupler with a radius of curvature R2.

The optical length of the resonator is represented as $L_b \equiv z_e + z_D + z_s$ if both of the thermal lenses are induced. The parameters g1 and g2 are determined by the complete expressions (1a, 1b) for the paraxial zone where the influences of both of the end- and side-pump are considered. For the peripheral zone the g-parameters are practically determined only by the optical power of the D_s lens ($D_e \approx 0$ in this zone).

We have analyzed several resonator configurations using the matrix approach to find out the hybrid pump power ranges corresponding to different position of the resonator in the stability diagram.

In the simulations we have used the parameters of the laser system studied in our physical experiments given in Section II.

The results of the simulation are presented in Fig. 1 as a 3D g-diagram showing the change in the position of the resonator in the stability diagram in terms of g1 and g2 (horizontal and vertical axes, respectively) against different values of product $g1_0 * g2_0$. Parameter $g1_0 * g2_0$ characterizes the resonator when the pump sources are off and the refractive power of thermally induced lenses is zero ($D_e = D_s = 0$). The values of this parameter are presented along the axis normal to plane formed by axes $\vec{g}_1$ and $\vec{g}_2$. The position of the corresponding plane of the g-diagram is determined by the values of $g1_0$ and $g2_0$. They depend only on the geometrical parameters of the resonator. For a particular case of a simple two-mirror cavity configuration it depends on the mirrors curvatures and the resonator's length.

Optics EXPRESS

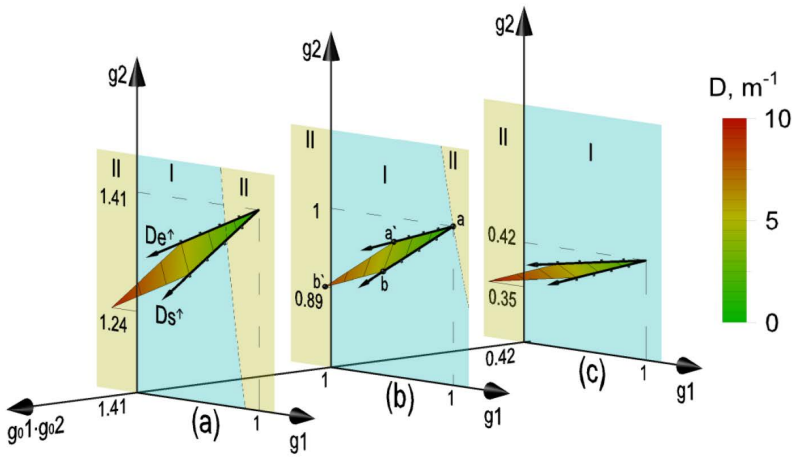

Fig. 1. Stability diagram of the plane-spherical resonator with two thermally induced lenses with variable optical powers D_e, and D_s. The output coupler's curvature radius is R2 = –500 mm (a), R2 = ∞ (b), R2 = 500 mm (c), resonator length is L_b = 135 mm. Zone I represents the stable region, zones II show the unstable regions for the resonator.

When the thermal lenses refractive power D_e and D_s changes (see destination of corresponding axes in the plane (a)), the current values of parameters g1 and g2 of the resonator will fall inside the limiting region. An example of the parallelogram-like regions formed by points a, a', b' and b is shown in the plane (b) of Fig. 1. The regions boundaries depend on the induced thermal lenses parameters and the position of the initial point "a". The latter is given by the pair of parameters $g1_0$ and $g2_0$. The 3D-diagram shown in Fig. 1 is plotted for resonators with a flat rear mirror ($R1^{-1} = 0$) and an output coupler with various radii of curvature, R2. The position and the shape of each region a-a'-b'-b are determined by the powers of the thermal lenses and the values of $g1_0*g2_0$. For illustrative purposes, the figure shows the planes corresponding to the unstable (a), flat (b), and stable (c) empty resonators. The optical power of the thermally induced lens corresponds to a color temperature whose scale is shown on the right. The color temperature within the closed a-a'-b'-b regions is introduced according to the total optical power supposed to be in a first assumption D ≈De + Ds. The lines inside the a-a'-b'-b regions correspond to the same values of total optical power of thermal lens (isochoric lines).

The diagrams similar to one shown in Fig. 1 are rather useful in making preliminary predictions for the changes in the state of the resonator with a given geometry upon changes in the absorbed pump power.

3. Experimental study of the Nd^{+3}YAG laser with diode hybrid pumping

3.1 Low-frequency pulsed pump (f<1 kHz)

At intended laser energy operation at low repetition rate (repetition rates of less than 1 kHz) leads to relatively low average pump power, and therefore the thermally induced lenses have low refractive power. In this case, the corresponding focal length of the lenses F_e and F_s is much longer than the resonator length L_b. The experimental setup is shown in Fig. 2.

Optics EXPRESS

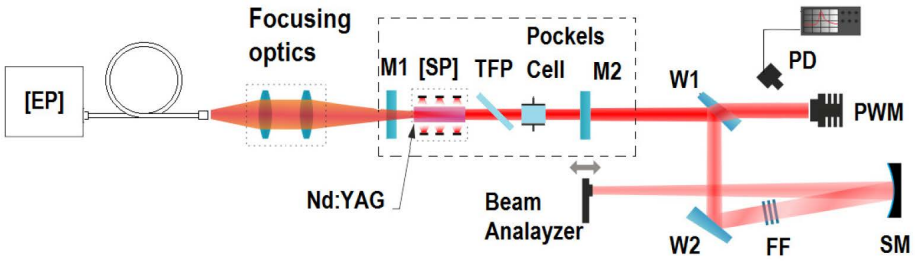

Fig. 2. [EP] – end-pump source; M1 – dichroic rear mirror (HR@1064 nm, HT@808 nm); [SP] – side-pump diode module with Nd:YAG active rod; TFP – thin film polarizer; M2 – output coupler (R_{oc} = 78%); W1, W2 – optical wedges; FF – optical filters ; SM – spherical mirror; PWM – power meter, PD – high-speed pin-photodiode with oscilloscope.

In the experimental setup the laser crystal was 60 mm long, 3 mm in diameter, 0.65% doped Nd:YAG rod, AR coated at 808 and 1064 nm. The crystal was end-pumped with a 70-W peak power Jenoptik (JOLD 70 QPXF 1L) multimode fiber-coupled laser diode operating at 808 nm. The radiation of the end-pumped system [EP] was introduced into the central part of the active rod along its axis by a focusing system through the dichroic rear mirror M1. Active rod of the laser was placed into standard side pumped laser chamber [SP] CEO 301C1 (4) equipped with 9 diode arrays (LDM) using 3 fold geometry of pumping (Fig. 3(a) with maximum total CW output power of 180 W. The resonator used plane rear mirror M1 and plane output coupler M2. The position of the focusing plane of the pump radiation was optimized using the criteria of the maximum averaged output power and maximum quality of the output beam with the hybrid pump. Thin film polarizer (TFP) and BBO crystal-based electro-optic switch deliver the Q-switching mode. The parameters of the resonator output emission were recorded with a power meter, a high-speed photodetector and oscilloscope. The thermal lens effect and the output beam quality were measured with a beam analyzer WinCam-D, an auxiliary He-Ne laser and spherical mirror SM.

Figure 3(a) shows the characteristics of the end-pump [EP] and side-pump [SP] modules used in the experiment. Figure 3(b) shows the output beam intensity distributions in the focal plane of the outer spherical mirror (11) when either the side-pump alone or the hybrid pump is used. In the case of the hybrid pump the measured M^2 parameter decreases more than two times compared to the side-pump configuration and it was about 1.15 at the maximum energy of the pump pulses.

The diagrams for the generated pulse's energy and duration on the end-pump module driving current for different levels of side pump peak power are presented in Fig. 3(c), 3(d). They were obtained in a pulsed-periodical pump mode with a pulse duration of 125 μs and a repetition rate of 100 Hz. The results show that in the absence of an end-pump, the maximum generated pulse energy is 1.5 mJ with pulse duration of 35 ns. The introduction of an additional pump into the paraxial zone of the active rod leads to the decrease of the pulse duration by 35-40% whereas the pulse energy increases up to 2.6 mJ.

Optics EXPRESS

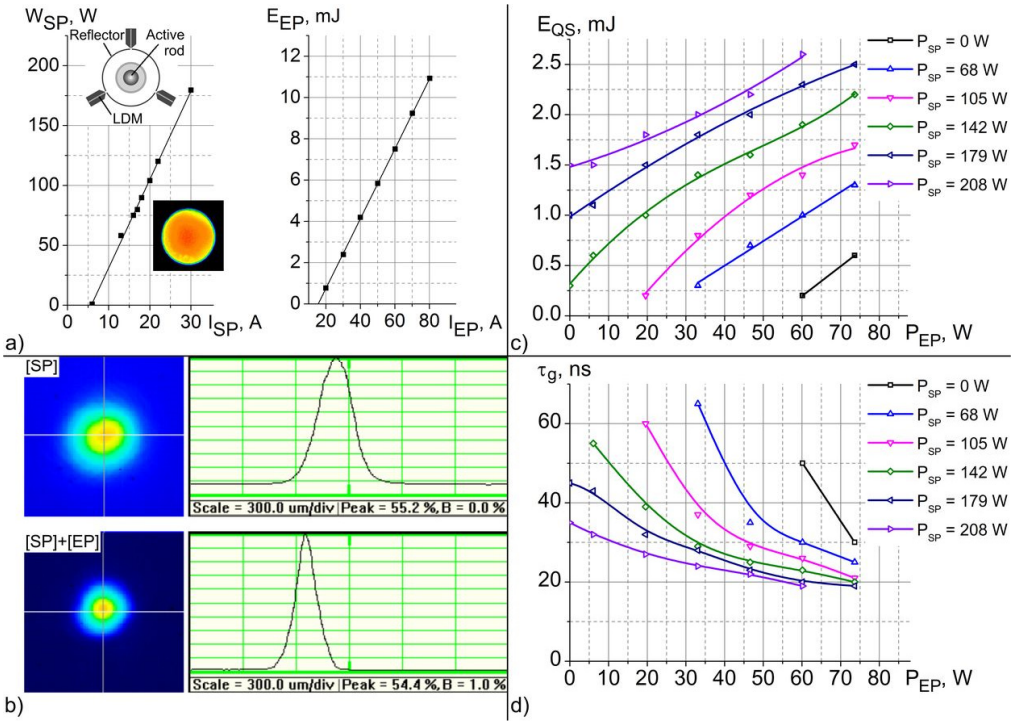

Fig. 3. a) Side pump scheme, transversal distribution of fluorescence in the active rod and power parameters of [SP] and [EP] systems (I_{SP}, I_{EP} are the side- and end pump systems working current values respectively; b) output beam intensity distributions for the side-pump (1) and hybrid pump (2) operation modes; c, d) pulse energy and duration vs end-pump peak power P_{EP} for different levels of side pump peak power P_{SP}.

A further increase of the output pulse energy was limited by the laser-induced damage of the antireflection-coated surfaces of the used intracavity optical components. In the absence of side-pump there was lasing at the fundamental (TEM_{00}) mode. The emission pulse width was close to the minimum achieved in the experiments. The output pulses energy was slightly above 0.5 mJ at the maximum current. The combination of the both pump sources provides larger gain factor in the paraxial zone of the active rod, which facilitates a more rapid lasing build-up at the lowest transverse mode. As it has been suggested earlier, the radiation in the fundamental mode acts as a seed for the further development of lasing and essentially determines both the pulse length and the intensity distribution of the output pulses.

3.2 Continuous wave pump operation mode

To increase the repetition rate and the average laser power, the hybrid pump scheme was used in a CW mode. In this case, strong effects of thermally-induced lenses and birefringence occur in the laser media.

The experimental setup is shown in Fig. 4. It is similar to that shown in Fig. 2. The difference is in the type of the end-pump source and the optical Q-switch, as well as in the choice of radii of curvature of the resonator mirrors. The latter was necessary due to the formation of two combined thermally-induced lenses with focal lengths comparable with the resonator length. The resonator configuration with a schematic representation of the thermally induced lenses is shown in Fig. 3.

The end-pump source was a fiber coupled module MU55-808 (SvetWheel LLC) with the central generation wavelength of 808 nm. This module has a threshold current of I_{thr} = 2A, maximum current of I_{max} = 8A, and a slope equal to 8W/A. The output optical fiber diameter was 200 μm and fiber numerical aperture was NA = 0.22. We used a focusing objective with

Optics EXPRESS

the same magnification (≈1). Quartz glass-based acousto-optical switch (AOS) with the carrier frequency of 50 MHz and an operating frequency up to 10 kHz was used for the Q-switch mode. The modulation depth was 35%. The level of losses introduced by the modulator was sufficient for the complete resonator switch-off between the pulses. AOSs of this type exhibit low sensitivity to thermally induced active rod birefringence. The dissipative losses in the resonator due to the radiation depolarization decreased from 35% (electro-optic modulator) to less than 1%.

The measured lasing build-up time in the paraxial zone of the active rod exceeded 650 ns at the maximum pump level. Thus, the change of an electro-optic switch for the acousto-optical modulator has no essential effect on the output pulse duration.

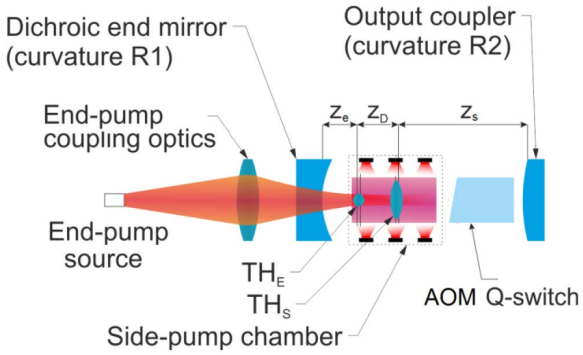

Fig. 4. Scheme of the laser with continuous hybrid pump. TH_E and TH_S – thermally induced lenses caused by end- and side pump radiation.

The radii of curvature for the output coupler were chosen to compensate the bifocal thermal lenses in the active rod (0.65%Nd:YAG, [100]). The optical power of the thermally induced lenses in the paraxial and the peripheral zones of the laser element can be managed via a change of the driving currents I_{EP} and I_{SP}, variation of the laser diodes temperature and the position of the active rod. All these parameters affect the radiation's caustic formation.

Figures 5(a) and 5(b) show the calculated boundaries of the g - parameters in the paraxial region of the resonator corresponding to the change in the end-pump power W_{EP} in the range 0-50W. The lines a-a', b-b' correspond to the side-pump power values of W_{SP} = 0 and 180 W, respectively. The lines a-b, a'-b' correspond to the limiting values of the end-pump of 0 and 50 W. The diagram corresponds to one of the planes in a 3D-diagram in Fig. 1 for the given radius of curvature of the convex output coupler mirror R2 = −500 mm used in the experiments.

In the absence of the side-pump (W_{SP} = 0), the paraxial zone of the resonator becomes stable at W_{EP} = 12 W (D ≈1.5 m^{-1}, I_{EP} = 2.2 A), then the resonator shifts to an unstable region at W_{EP} = 39 W (D ≈5.5 m^{-1}, I_{EP} = 6 A) (see line a-a' in Fig. 5(a)). The peripheral zone of the resonator becomes stable upon increase of the side-pump (see the line a-b in Fig. 6(a) only at W_{SP} = 90 W (D ≈1.7 m^{-1}, I_{SP} = 18 A).

In the optimal operation mode of the investigated laser with a hybrid pump, the peripheral zone of the resonator is in the unstable region (magnification coefficient M ≈1.45, see Fig. 5(b)) close to the stability region's boundary (point A0 in Fig. 5(a)). Thus, the gain coefficient in the peripheral zone is nearly own lasing threshold.

Optics EXPRESS

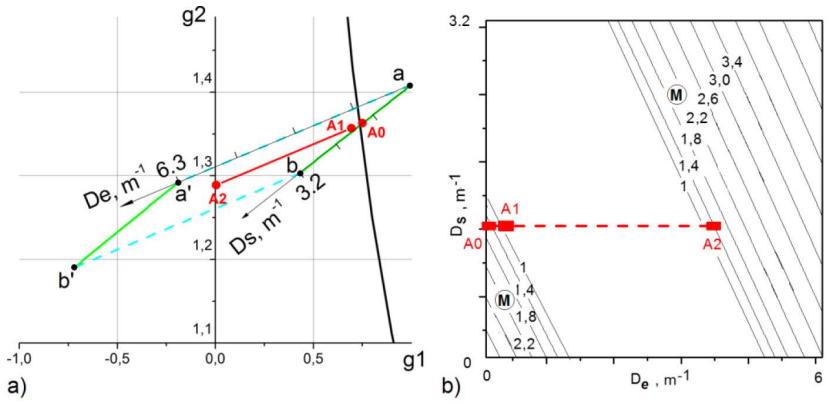

Fig. 5. Calculated dependences for the resonator with an output coupler radius of curvature R2 = –500 mm: a) g1g2 stability diagram; b) Magnification coefficient M for the resonator in the unstable configuration region. The area without isolines corresponds to the stable generation regime (M = 1).

At the same time, the paraxial zone of the resonator is within the stability region for end-pump power in the range of W_{EP} = 2.5-28 W (D = 1.7-5.5 m^{-1}, see points A1-A2 in Fig. 5(a)). Under the given conditions, the generation starts in the paraxial zone of the active rod with the maximum gain coefficient. Due to the spatial distribution of the gain coefficient and the smallness of the Fresnel number, the quality of the beam is high. Then as the generation pulse develops, the radiation starts filling up the peripheral zone due to diffraction and configuration of unstable resonator. Thus the "seed" radiation from the paraxial zone is further amplified in the peripheral one. The quality of the beam gets worse in the course but remains high enough as compared to that of a typical side-pump (Fig. 6).

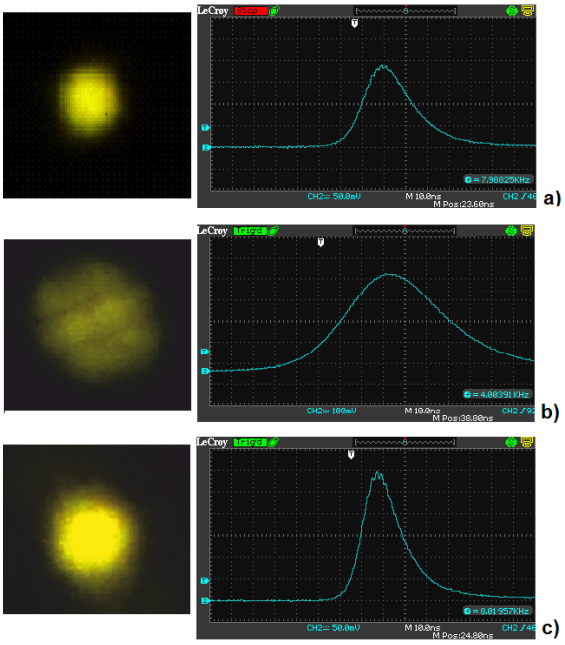

Fig. 6. Transverse intensity distribution and generated pulse temporal profile for generation at 8 kHz; a) end-pump (I_{EP} = 5 A), average output power W_g = 2.4 W, τ_g = 22 ns; b) side-pump (I_{SP} = 24 A), W_g = 19 W, τ_g = 50 ns; c) side + end-pump (I_{EP} = 6 A, I_{SP} = 24 A), W_g = 21 W, τ_g = 18 ns.

Optics EXPRESS

The output characteristics of the laser generator with a continuous hybrid pump for the chosen combination of the resonator parameters and pump power are given in Fig. 7.

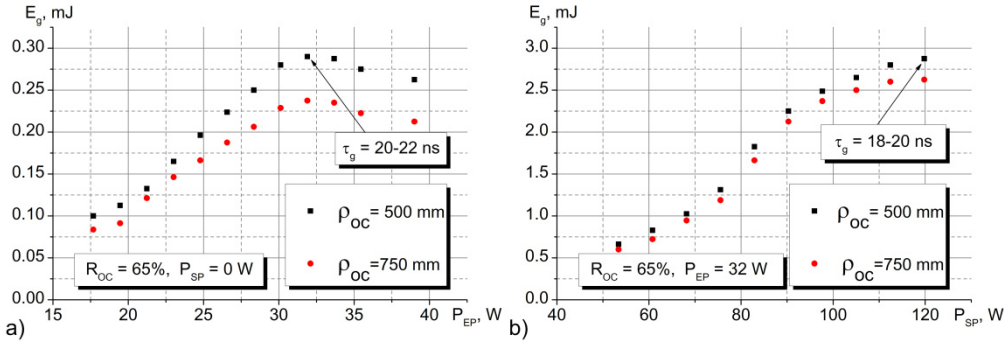

Fig. 7. Experiment using CW end and side pumping -Stage II. Results at Q-switched repetition rate f = 8 KHz, a) Output pulse energy vs end-pump power P_{EP} ($P_{EP} = W_{EP}$ in the case of CW pumping); b) pulse energy vs side-pump power P_{SP} at P_{EP} = 32 W corresponding to the max output energy in Fig. 7(a).

4. Conclusion

It has been shown that using a combined diode end-pump and side-pump in a compact solid-state Q-switched lasers is beneficial for achieving both a high average power, which is typical for side-pumped lasers, and a high emission brightness and peak power, pertaining to end-pumped lasers. The stability diagram of the resonator with two cases of thermal lenses has been investigated. A laser oscillator with a single Nd:YAG 3x60 mm active rod using simultaneously an end- and a side-pump has been shown to produce pulses with energies of up to 3 mJ, pulse duration below 20 ns, repetition rate up to 8 kHz at $M^2<2$, and average power exceeding 20 W. The laser is intended as seed generator in XUV radiation sources based on laser plasma using the pre-pulse technique [20].

Funding

Bulgarian National Science Fund (DN 08/05).

Acknowledgments

We acknowledge support from the Ministry of Education & Science of the Russian Federation for Research at the ITMO University. We extend our gratitude to E.N. Ofitserov for his aid in the performing the experiments and to A.V. Erofeev for the fruitful discussions.